Image quality improvement of polygon computer generated holography

Xiao-Ning Pang, Ding-Chen Chen, Yi-Cong Ding, Yi-Gui Chen, Shao-Ji Jiang, and Jian-Wen Dong*

School of Physics and Engineering, and State Key Laboratory of Optoelectronic Materials and Technologies, Sun Yat-sen University, Guangzhou, 510275, China

** dongjwen@mail.sysu.edu.cn*

Abstract: Quality of holographic reconstruction image is seriously affected by undesirable messy fringes in polygon-based computer generated holography. Here, several methods have been proposed to improve the image quality, including a modified encoding method based on spatial-domain Fraunhofer diffraction and a specific LED light source. Fast Fourier transform is applied to the basic element of polygon and fringe-invisible reconstruction is achieved after introducing initial random phase. Furthermore, we find that the image with satisfactory fidelity and sharp edge can be reconstructed by either a LED with moderate coherence level or a modulator with small pixel pitch. Satisfactory image quality without obvious speckle noise is observed under the illumination of bandpass-filter-aided LED. The experimental results are consistent well with the correlation analysis on the acceptable viewing angle and the coherence length of the light source.

OCIS codes: (090.0090) Holography; (090.1760) Computer holography; (090.2870) Holographic display.

References and links

1. J.-H. Park, K. Hong, and B. Lee, "Recent progress in three-dimensional information processing based on integral imaging," Appl. Opt. **48**(34), H77–H94 (2009).
2. J. Hong, Y. Kim, H.-J. Choi, J. Hahn, J.-H. Park, H. Kim, S.-W. Min, N. Chen, and B. Lee, "Three-dimensional display technologies of recent interest: principles, status, and issues [Invited]," Appl. Opt. **50**(34), H87–H115 (2011).
3. J. Geng, "Three-dimensional display technologies," Adv. Opt. Photonics **5**(4), 456–535 (2013).
4. H. Nishi, K. Matsushima, and S. Nakahara, "Rendering of specular surfaces in polygon-based computer-generated holograms," Appl. Opt. **50**(34), H245–H252 (2011).
5. W. Lee, D. Im, J. Paek, J. Hahn, and H. Kim, "Semi-analytic texturing algorithm for polygon computer-generated holograms," Opt. Express **22**(25), 31180–31191 (2014).
6. S.-C. Kim and E.-S. Kim, "Fast computation of hologram patterns of a 3D object using run-length encoding and novel look-up table methods," Appl. Opt. **48**(6), 1030–1041 (2009).
7. N. Masuda, T. Ito, T. Tanaka, A. Shiraki, and T. Sugie, "Computer generated holography using a graphics processing unit," Opt. Express **14**(2), 603–608 (2006).
8. J. W. Goodman, *Introduction to Fourier Optics* (McGraw-Hill, 1996).
9. Y. Ichihashi, H. Nakayama, T. Ito, N. Masuda, T. Shimobaba, A. Shiraki, and T. Sugie, "HORN-6 special-purpose clustered computing system for electroholography," Opt. Express **17**(16), 13895–13903 (2009).
10. H. Kim, J. Hahn, and B. Lee, "Mathematical modeling of triangle-mesh-modeled three-dimensional surface objects for digital holography," Appl. Opt. **47**(19), D117–D127 (2008).
11. L. Ahrenberg, P. Benzie, M. Magnor, and J. Watson, "Computer generated holograms from three dimensional meshes using an analytic light transport model," Appl. Opt. **47**(10), 1567–1574 (2008).
12. Y.-Z. Liu, J.-W. Dong, Y.-Y. Pu, B.-C. Chen, H.-X. He, and H.-Z. Wang, "High-speed full analytical holographic computations for true-life scenes," Opt. Express **18**(4), 3345–3351 (2010).
13. Y.-Z. Liu, J.-W. Dong, Y.-Y. Pu, H.-X. He, B.-C. Chen, H.-Z. Wang, H. Zheng, and Y. Yu, "Fraunhofer computer-generated hologram for diffused 3D scene in Fresnel region," Opt. Lett. **36**(11), 2128–2130 (2011).
14. J. Amako, H. Miura, and T. Sonehara, "Speckle-noise reduction on kinoform reconstruction using a phase-only spatial light modulator," Appl. Opt. **34**(17), 3165–3171 (1995).

#241240 Received 18 May 2015; revised 4 Jul 2015; accepted 11 Jul 2015; published 15 Jul 2015

15. K. Matsushima, "Computer-generated holograms for three-dimensional surface objects with shade and texture," Appl. Opt. **44**(22), 4607–4614 (2005).
16. J. W. Goodman, *Speckle Phenomena in Optics* (Roberts & Company, 2006).
17. E. Moon, M. Kim, J. Roh, H. Kim, and J. Hahn, "Holographic head-mounted display with RGB light emitting diode light source," Opt. Express **22**(6), 6526–6534 (2014).
18. Y. Zhao, L. Cao, H. Zhang, and Q. He, "Holographic display with LED illumination based on phase-only spatial light modulator," Proc. SPIE **8559**, 85590B (2012).
19. F. Yaraş, H. Kang, and L. Onural, "Real-time phase-only color holographic video display system using LED illumination," Appl. Opt. **48**(34), H48–H53 (2009).
20. T. Ito, T. Shimobaba, H. Godo, and M. Horiuchi, "Holographic reconstruction with a 10- mum pixel-pitch reflective liquid-crystal display by use of a light-emitting diode reference light," Opt. Lett. **27**(16), 1406–1408 (2002).
21. K. Matsushima and T. Shimobaba, "Band-limited angular spectrum method for numerical simulation of free-space propagation in far and near fields," Opt. Express **17**(22), 19662–19673 (2009).
22. K. Matsushima, H. Schimmel, and F. Wyrowski, "Fast calculation method for optical diffraction on tilted planes by use of the angular spectrum of plane waves," J. Opt. Soc. Am. A **20**(9), 1755–1762 (2003).
23. Y. Pan, Y. Wang, J. Liu, X. Li, and J. Jia, "Fast polygon-based method for calculating computer-generated holograms in three-dimensional display," Appl. Opt. **52**(1), A290–A299 (2013).
24. K. Matsushima, "Shifted angular spectrum method for off-axis numerical propagation," Opt. Express **18**(17), 18453–18463 (2010).

1. Introduction

Three-dimensional (3D) display techniques providing vivid reconstruction of 3D scenes have attracted lots of research interest [1–3]. Holography is one of promising way for 3D display with binocular parallax and visual comfort due to the ability to reconstruct complex wavefront of the recording light field. The light field of virtual 3D models, which compose of triangles with texture [4, 5] or points with different intensities [6, 7], can be encoded into computer-generated hologram (CGH) using Rayleigh-Sommerfeld diffraction [8]. Light field on hologram plane is the linear superposition of each computing unit. In point-based methods, a number of computing units are needed to guarantee satisfactory vivid effect [9], while less are needed to obtain similar results for the same scene in triangle-based methods [10, 11]. In our previous proposal, an analytical computation method was derived to generate phase-only hologram for triangle-based model [12, 13]. However, undesirable fringes were introduced in the reconstructed image due to the subdivision of each triangle in textured model. A new method without extra subdivision is necessary for the improvement of reconstructions.

Laser is a good choice as light source for holographic imaging due to its high spatial and temporal coherence. However, the inevitable noise in the reconstructed image has constrained further applications in laser-based 3D holographic display. Speckle noise in laser-based holographic display system mainly results from two reasons. One is known as numerical noise from the random phase introduced in the encoding process of phase-only CGH [14, 15]. Another comes from the phase fluctuations of coherent light beam when it transmits through or reflects off a diffusive plane [16]. Using LED is an alternative way to smooth speckle noise. Many groups have applied LED into their holographic systems and the relevant effects have been discussed [17–20]. Although speckle noise in reconstructed images can be smooth due to low coherence of LED, the information of signal is also lost. Therefore, the imaging quality, especially sharpness of the object boundary, becomes another problem for LED-illuminated holographic imaging. LED reconstruction is far from satisfactory. Quantitative analysis of the restriction on the high-quality image area for LED holographic reconstruction has been few of study yet.

In this paper, we propose a method on encoding the CGH for polygonal model by applying fast Fourier transform (FT) instead of analytical FT. Such method enables to avoid the subdivision of each polygon, and as a result, fringes inside the reconstructed triangle are gone and vivid objects with smooth surfaces appear. We also analyze the high quality imaging area as a function of the coherence length of the light source and the pixel pitch of the modulator. We find that laser is not necessary for modulator-based holographic image. The image with satisfactory fidelity and sharp edge can be reconstructed by either a LED with modified

#241240 Received 18 May 2015; revised 4 Jul 2015; accepted 11 Jul 2015; published 15 Jul 2015

coherence level or modulator with small pixel pitch. The experimental results are well consistent with the above analysis.

2. Elimination of undesirable fringes by fast Fourier transform

For triangle-based model, the diffraction field of an arbitrary tilted triangle can be evaluated by two different ways. One is called spectrum-domain method, e.g. angular spectrum method. In this method, the complex field distribution of the object plane can be considered as summation of various spatial Fourier components which are plane waves traveling in different directions away from the object plane. The field amplitude at any other point on hologram plane can be calculated by adding the contributions of these plane waves, taking account of the phase shifts they have undergone during propagation [8]. Both FFT and inverse FFT should be performed to obtain the diffraction field. Many researchers use this method to evaluate the diffraction field of tilted plane [21–23]. Several modified versions have been proposed, such as band-limited angular spectrum method [21] and shifted angular spectrum method [24].

In this paper, we employ the spatial-domain method, e.g. direct Fresnel integral calculation method which is based on the first Rayleigh-Sommerfeld solution. The diffraction field on the hologram plane directly relates to the spatial distribution of the object field. A Fresnel approximation is introduced into the integral to make it easy to evaluate. The Fourier transform is used once a time in the calculation process. In our previous proposal, a full analytical computational method was developed to generate hologram from textured triangle-based model [12]. The diffraction field of the whole object is obtained by the linear combination of that of each triangle. Using Fraunhofer diffraction integral, the diffraction field of each triangle on the hologram plane can be expressed as

$$O_H(x_H, y_H) = \frac{\exp[ik(z_c + r_0)]}{i\lambda r_0} \mathcal{F}\{O_o(x_l, y_l)\}, \tag{1}$$

where λ is wavelength in vacuum and $k = 2\pi/\lambda$. z_c is the position of the triangular mass center in z direction, (x_l, y_l) is the local coordinate of triangle, r_0 is the distance between the triangular mass center and the hologram pixel. $\mathcal{F}\{O_o(x_l,y_l)\}$ is the Fourier transform of a single triangle, which can be obtained using affine transform according to the Fourier transform $\mathcal{F}_\Delta$ of a given right triangle with vertices in the points of (0,0), (1,0), (1,1),

$$\mathcal{F}\{O_o(x_l, y_l)\} = (a_{22}a_{11} - a_{12}a_{21}) \exp(-\mathrm{i}\, 2\pi \frac{a_{13}x'_H + a_{23}y'_H}{\lambda r_0}) \mathcal{F}_\Delta(\frac{a_{11}x'_H + a_{21}y'_H}{\lambda r_0}, \frac{a_{12}x'_H + a_{22}y'_H}{\lambda r_0}). \tag{2}$$

Here, a_{ij} (i = 1, 2, j = 1, 2, 3) are the elements of affine transform matrix. See more detail formulism in Refs. 12 and 13. For physics point of view, it suggests that only the analytical Fourier transform of the given right triangle is needed for the whole scene. However, it is not a good choice when achieving the vivid reconstruction of textured scene. Fine subdivision should be applied in each triangle in order to ensure constant intensity in each sub-triangle. This is impractical for real time holographic video, in particular when the texture is much more complicated, as the number of sub-triangles will increase significantly. Even if the texture is too simple to subdivide, there are still redundant fringes in the reconstructed image [see e.g. Figure 1(a) and 1(b)]. Such redundancy is originated from the high-spatial-frequency components when the triangle is not so small. Most of the power remains on the edges of each sub-triangle, leading to lack of light field inside the mesh frame. To fix this problem, a random phase is added into the complex profile of each triangle to smooth the spectrum on the hologram since only the intensity of the reconstruction is of concern. Fast Fourier transform is used instead of analytical Fourier transform. A 3D scene of two rectangular planes with texture (alphabets A and B), which locate at the position 800 mm and 1100 mm away from hologram

#241240 Received 18 May 2015; revised 4 Jul 2015; accepted 11 Jul 2015; published 15 Jul 2015

plane, respectively, is used to illustrate the difference between analytical FT and fast FT methods. Numerical reconstructions of hologram encoded using analytical method are shown in Figs. 1(a) and 1(b). Each triangle is divided into tens of small sub-triangles. However, only the edges (high-spatial-frequency components) of each sub-triangle can be observed, while a relatively smooth rectangle is obtained using fast Fourier transform method shown in Figs. 1(c) and 1(d). When the reconstruction distance is 800 mm, the rectangle with character A is in focus and that with character B is out of focus, as shown in Figs. 1(a) and 1(c). But it is vice versa when the reconstruction distance is 1100 mm.

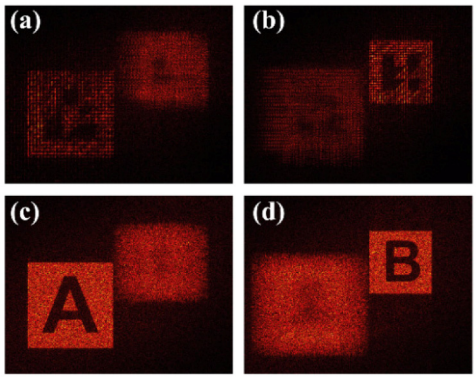

Fig. 1. Comparison of numerical reconstructed image using (a)-(b) analytical Fourier transform and (c)-(d) fast Fourier transform method. The rectangle sizes are 10 × 10 mm. The rectangle with texture of character A locates at 800 mm away from the hologram plane while that with character B locates at 1100 mm. The rectangles are subdivided to tens of triangles in (a) and (b), while not in (c) and (d). Note that the unexpected fringes can be seen in (a) and (b) due to the use of analytical method, while a smooth rectangle in (c) and (d) is reconstructed by fast Fourier transform. When the reconstruction distance is 800 mm, the rectangle with character A is in focus and that with character B is out of focus in (a) and (c), and vice versa.

3. Quantitative analysis on LED illuminated holographic imaging

In this section, we will investigate the fidelity of holographic imaging area in LED illuminated holographic system. Figure 2 shows the schematic diagram the LED illuminated holographic system. Light emitted from LED source is collimated after spatial filter and convex lens. Hologram is uploaded to a phase-only spatial light modulator (SLM). A real image is then reconstructed on the image plane. Imaging quality at point P relies on the interferences among all the beams that propagate from SLM pixels to point P. The coherence length of the light source is $L_c = \lambda^2/\Delta\lambda$ and the optical path difference (OPD) of beams from different pixels denotes as ΔL. Here, $\Delta\lambda$ is the bandwidth of light source. The OPD between two beams which propagates from two marginal pixels on SLM, denoted as A and B respectively, is $\Delta L \approx np\sin\varphi \approx npx/r$, where r is the distance between the SLM and the imaging plane, x is the distance between imaging point P and the optical axis, n is the total number of pixels along the x direction and p is the pixel pitch of SLM. If these two beams are completely coherent in between, the coherence among all the beams from other positions on the SLM plane to point P can be guaranteed.

In order to determinate the size of high quality imaging area, the relation between the coherent length of light source and the OPD of the system should be considered. In classical optics, the relation between OPD and coherent length is important on interference. The coherence length of the light source in laser-illuminated holographic imaging system is always several orders of magnitude larger than the maximal OPD of the system, and thus the imaging quality is independent on the lateral position of reconstructed image. For example, the coherence length of laser with the wavelength of λ = 532 nm and the bandwidth of $\Delta\lambda_{\text{Laser}} = 10^{-4}$ nm is L_c(laser) ≈2.83 m. On the other hand, the SLM has the number of horizontal pixels

#241240 Received 18 May 2015; revised 4 Jul 2015; accepted 11 Jul 2015; published 15 Jul 2015

of n = 1920 and the pixel pitch of p = 8 μm. For the reconstruction distance of r = 800 mm and the maximal transverse displacement (along the x direction) of image area in the first diffraction order of $x_{max} = \lambda r/2p$ = 26.6 mm, the maximal OPD of the system is $\Delta L_{max} \approx 5.1 \times 10^{-4}$ m, much less than the coherence length of laser, i.e. $\Delta L_{max} \ll L_c$(laser). Thus, the factor $R = \Delta L_{max}/L_c$(laser) $\ll 1$. It indicates that human eyes cannot tell the difference between the reconstructed patterns at the center of the screen and those locate x_{max} away from the center along the transverse (x) direction, as shown in Fig. 2.

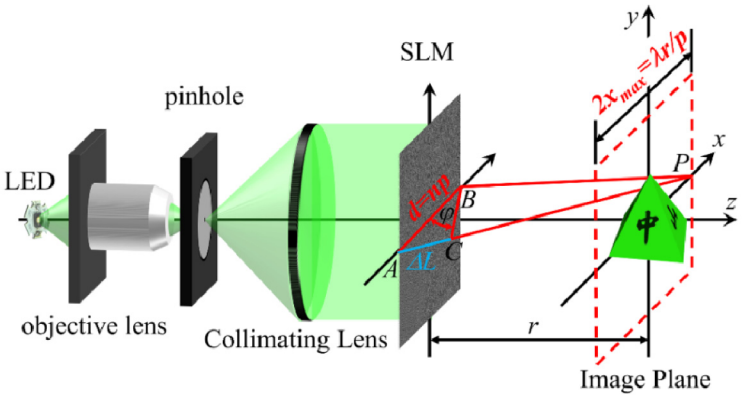

Fig. 2. Schematic diagram of LED-illuminated holographic system. P is an arbitrary point in the imaging area, r is the distance between reconstructed image and hologram, AB = np is the transverse length of SLM, where n is number of pixels, p is the pixel pitch. ΔL is the OPD between AP and BP. x_{max} is the maximal transverse displacement of image area in the first diffraction order.

However, it is not the case of LED-illuminated system. When it comes to LED light source, the coherence length decreases strikingly. The representative bandwidth of LED is $\Delta\lambda_{\mathrm{LED}}$ = 40 nm, and the corresponding coherence length is L_c(LED)≈7.08×10^{-6} m. The coherent length of LED is even less than the maximal OPD, i.e. L_c(LED) $\ll$ ΔL_{max}. It implies that complete coherence cannot be satisfied within the whole image plane in LED holographic reconstruction. Extra restriction on imaging region needs to be introduced. The size of high quality imaging area, which relates to OPD, should be investigated to modify the relation between the OPD and the coherent length. An experiment is performed to obtain the factor R in LED illuminated system. A pyramid is reconstructed and moved vertically by adding phase shift. The quality of image becomes worse with the position of image from zero-order beam changing. The red circle with image distance of x≈15.0 mm in the figures indicate the observers' maximal blur tolerance. Then the factor $R = \Delta L/L_c$(LED)≈10. For simply, a constant is divided to make the ratio to be unity, i.e. $R = \Delta L/(\alpha L_c(\mathrm{LED})) = 1$, where α = 10. So an empirical image quality factor R is modified as,

$$R = \Delta L/(10L_c) = npx/(10rL_c) = np\theta/(10L_c). \quad (3)$$

According to Eq. (3), the imaging quality is guaranteed only in the area that R<1 is satisfied, and θ is the acceptable viewing angle ($\theta = x/r$). In order to enlarge the acceptable angle, one can increase the coherence length of light source L_c and reduce the pixel pitch p. Numerical simulations of image quality factor are carried out in order to investigate the correlation among the acceptable angle, the coherence length and the pixel pitch. Figure 3(a) shows that the quality factor changes with the position on image plane. The red circle is the boundary of high image quality region, indicating that the reconstructed image can be clearly observed only if it locates within the red circle. In Fig. 3(b), we demonstrate the relationship between the acceptable angle and the pixel pitch in a given coherence length when R = 1. If the pixel

#241240 Received 18 May 2015; revised 4 Jul 2015; accepted 11 Jul 2015; published 15 Jul 2015

dimension of the SLM reduces, the acceptable angle will increase and dramatically enlarges when the pixel pitch is smaller than 2 μm. Another way to enlarge the acceptable angle is to enlarge the coherence length of the light source. As the filling factor of the SLM cannot reach to 100%, the distance between reconstructed images of adjacent diffractive orders is fixed. Although larger coherence length results in wider acceptable angle, i.e. wider region on the target plane, the reconstructed images of different orders may overlap with each other. In modulator-based holographic system, the yellow solid curve in Fig. 3(b) for the case of the 100 μm coherence length fits well with the green dash curve for the SLM limit. It suggests that the acceptable angle will not be enlarged even if the coherence length of light source is longer than 100 μm. Figure 3(c) shows that the acceptable viewing angle increases with the coherence length. Comparison between two typical commercial pixel pitches of SLM is shown in Fig. 3(c). If the coherence length is fixed at L_c = 5 μm, the acceptable angle increases twice when the pixel size falls to about one half. If the coherence length further increases to 30 μm, the acceptable angle will become 10 times of the initial value, which is an effective way to bring LED light source into holographic display system.

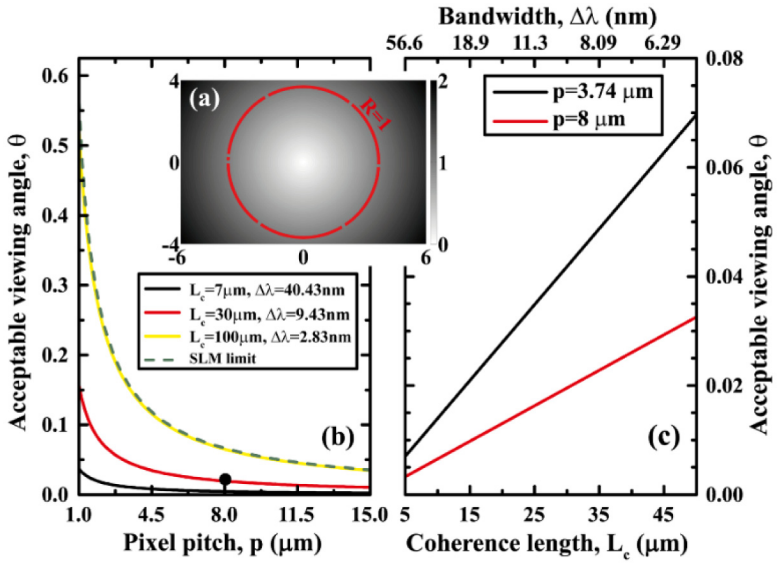

Fig. 3. (a) Image quality factor R described by Eq. (3), changes with the position of image point. Image quality can be guaranteed only if the reconstructed image locates within the red circle. (b) Acceptable angle increases with the decrease of the pixel pitch, when the coherence length is fixed. (c) Acceptable angle as a function of the coherence length for a given pixel pitch.

According to the analysis above, the quality of reconstructed image varies with the position of image. A scene with a pyramid is used to illustrate the effect on image qualify with the change of its position. The position of reconstructed image is changed by adding extra linear phase shift onto the hologram. The system is illuminated by LED with a 9.6 nm bandwidth filter. Note that the distance between the reconstruction and the hologram plane is 800 mm. The reconstructed images are first projected on a diffuse plane and then captured using camera. The results are illustrated in Fig. 4. The bright spots at the bottom of Figs. 4(a)-4(d) are the zero-order light. Sharp edges can be observed when the images locate near the zero-order light [Figs. 4(a) and 4(b)], while they blur for those cases in Figs. 4(c) and 4(d). The intensity profiles of neighborhood around the edge of the model [white segments in Figs. 4(a)-4(d)] are shown in Fig. 4(e). The curve corresponding to Fig. 4(b) falls down quickly indicating a sharp edge, while the curve of Fig. 4(d) changes slowly and thus the edge of model blurs. Therefore, for LED-illuminated holographic system, due to the low coherence of light source, imaging

#241240 Received 18 May 2015; revised 4 Jul 2015; accepted 11 Jul 2015; published 15 Jul 2015

quality relies strongly on the position of image. Images locate on central part are much better than those on the periphery for naked eye observation.

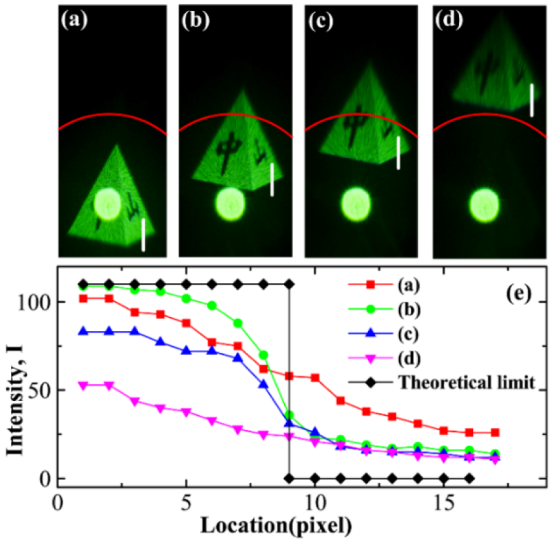

Fig. 4. Analysis on the imaging quality at different locations on the image plane. Experimental results of the same model are shown in (a)-(d). Extra linear phase is added to the modulator in order to shift the image away from the zero-order light, and sharp edge of the model can be seen only on the patterns near the optical axis. The red circles indicate that R = 1. (e) Intensity profiles of the white segments in (a)-(d) are plotted and the best result is obtained for the curve of (b) because of the minimal distance between the model and optical axis among these three cases.

Figure 3 implied that the acceptable viewing angle for naked LED (L_c≈7 μm) is very limited (θ ≈5 × 10^{-3} rad) when the pixel pitch of SLM is 8 μm. In order to improve the acceptable viewing angle, a pyramid with height of 15 mm is used to investigate the relation between the acceptable viewing angle and the bandwidth in LED-illuminated holographic system. Different band-pass filters are introduced into the optical setup in order to mimic different bandwidth of light source. The reconstructed images for LED with the bandwidths of 27 nm, 18 nm and 9.6 nm, as well as the laser illumination with the bandwidth of 10^{-4} nm, are illustrated in Fig. 5. It is found that sharp boundary is clearly to be seen in laser reconstruction scene, but serious speckle appears on and around the pyramid [Fig. 5(a)]. For the naked LED case, the reconstructed image is seriously blurred because the whole image exceeds the corresponding high quality imaging area [Fig. 5(d)]. After employing band-pass filters, the coherence length increases and the acceptable region is also enlarged, so that the reconstructed images of the same model obtain better results than that of naked LED [Fig. 5(b) and 5(c)]. Speckle contrast ratio is used to estimate the quality of reconstructed image, which is defined as follow [16],

$$C = \sigma_I / \bar{I} = \sqrt{\frac{1}{N}\sum_{i=1}^{N}(p_i - \bar{I})^2} \Big/ \bar{I}. \tag{4}$$

Here, $\bar{I}$ is the average intensity of all pixels, p_i is the intensity of the ith pixel and N indicates the total number of pixels in the information region. We randomly choose an area in reconstructed image [area inside the red rectangle in Figs. 5(a)-5(d)] to calculate the speckle contrast ratio. The results are plotted in Fig. 5(e) with red dots. It is obvious that the speckle noise reduces when the bandwidth rises. The black solid curve in Fig. 5(e) is the numerical simulation result. In the simulation, the spectrum of the light source is assumed to be rectangular profile with

#241240 Received 18 May 2015; revised 4 Jul 2015; accepted 11 Jul 2015; published 15 Jul 2015

random initial phase for each wavelength. The final reconstructed image is the superposition of the reconstructed images with different wavelengths. As shown in Fig. 5(e), the numerical speckle contrast ratio inside the red frame of the reconstructed image decreases with the bandwidth, consistent with the experimental results. It is a tradeoff between the bandwidth of light source and the quality of reconstructed image. Smaller bandwidth of light source has better coherence to provide sharper boundary while larger speckle contrast ratio. For the studied holographic system, light source with the bandwidth of 9.6 to 18 nm can provide satisfactory image quality without obvious speckle noise.

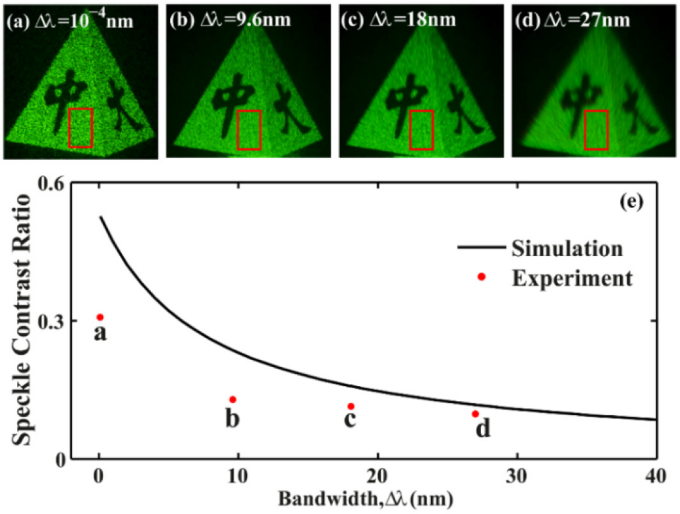

Fig. 5. Analysis on the influence of bandwidth of the light source. Experimental results employing (a) laser ($\Delta\lambda = 10^{-4}$nm), (b) LED with filter (9.6nm), (c) LED with filter (18nm) and (d) naked LED without filter ($\Delta\lambda$ = 27nm) are shown. Speckle contrast ratios of (a)-(d) are calculated and numerical simulation are carried out in (e). Note that there is a proper bandwidth of light source for the holographic system, which keeps imaging quality and speckle noise in good balance.

4. Conclusion

We propose a new method of phase-only CGH for textured polygon-based model by introducing fast Fourier transform instead of analytical diffraction computation. Such method cannot only avoid the subdivision of each polygon, but also eliminate the unexpected fringes inside the reconstructed image. High quality imaging area is investigated as a function of the coherence length of the light source and the pixel pitch of SLM. The acceptable angle is used to describe the image quality. The image with satisfactory fidelity and sharp edge can be reconstructed by either a LED with modified coherence degree of freedom or SLM with small pixel pitch. Experimental results show agreement with the above analysis. In addition, there exists a proper light source that is able to keep image quality and speckle noise in a good balance.

Acknowledgments

This work is supported by grants of Natural Science Foundation of China (61235002).

#241240 Received 18 May 2015; revised 4 Jul 2015; accepted 11 Jul 2015; published 15 Jul 2015